Comparison of *O*-(2-^{18}F-Fluoroethyl)-L-Tyrosine PET and 3-^{123}I-Iodo-α-Methyl-L-Tyrosine SPECT in Brain Tumors

Dirk Pauleit, MD[1,2]; Frank Floeth, MD[3]; Lutz Tellmann, BSc[4]; Kurt Hamacher, PhD[5]; Hubertus Hautzel, MD[1,2]; Hans-W. Müller, MD[2]; Heinz H. Coenen, PhD[5]; and Karl-J. Langen, MD[4]

[1]Clinic for Nuclear Medicine, Research Center Jülich, Jülich, Germany; [2]Department of Nuclear Medicine, Heinrich-Heine-University, Düsseldorf, Germany; [3]Department of Neurosurgery, Heinrich-Heine-University, Düsseldorf, Germany; [4]Institute of Medicine, Research Center Jülich, Jülich, Germany; and [5]Institute of Nuclear Chemistry, Research Center Jülich, Jülich, Germany

The aim of this study was to compare PET with *O*-(2-^{18}F-fluoroethyl)-L-tyrosine (^{18}F-FET) and SPECT with 3-^{123}I-iodo-α-methyl-L-tyrosine (^{123}I-IMT) in patients with brain tumors. **Methods:** Twenty patients with a suspected brain tumor were investigated by ^{18}F-FET PET, ^{123}I-IMT SPECT, and MRI within 3 wk. Region-of-interest analyses were performed on coregistered PET/SPECT/MRI images and the tumor-to-brain ratio (TBR), muscle-to-brain ratio (MBR), cerebellum-to-brain ratio (CerBR), and sinus-to-brain ratio (SBR) were calculated. In addition, the presence of tumor and the discrimination of anatomic structures on ^{18}F-FET PET and ^{123}I-IMT SPECT images were visually determined by 3 observers who were unaware of clinical data. **Results:** The TBR of ^{18}F-FET and ^{123}I-IMT uptake in cerebral tumors showed a highly significant correlation ($r = 0.96$; $P < 0.001$). In the visual analysis for the presence or absence of tumors, no differences for ^{123}I-IMT SPECT and ^{18}F-FET PET were found in 19 of 20 patients; in one patient a low-grade glioma was only identified on ^{18}F-FET PET images but not on ^{123}I-IMT SPECT images. The contrast between tumor and normal brain was significantly higher in ^{18}F-FET PET (TBR, 2.0 ± 0.9) than in ^{123}I-IMT SPECT (TBR, 1.5 ± 0.5). The discrimination of anatomic structures yielded a significantly better score on ^{18}F-FET PET images (rating score, 2.6 ± 0.9) compared with ^{123}I-IMT SPECT images (rating score, 1.7 ± 0.9). The uptake of ^{18}F-FET in the muscles was significantly higher compared with ^{123}I-IMT (MBR ^{18}F-FET, 1.4 ± 0.3; MBR ^{123}I-IMT, 0.6 ± 0.2; $P < 0.001$) and ^{18}F-FET demonstrated a significantly higher blood-pool radioactivity than ^{123}I-IMT (SBR ^{18}F-FET, 1.3 ± 0.2; SBR ^{123}I-IMT, 0.8 ± 0.2; $P < 0.001$). **Conclusion:** The significant correlation of the TBRs of ^{18}F-FET and ^{123}I-IMT indicates that clinical experiences of brain tumor diagnostics with ^{123}I-IMT SPECT might be valid for ^{18}F-FET PET although substantial differences of the physiologic behavior were identified in extracerebral tissue. As ^{18}F-FET PET allows improved discrimination of anatomic structures and the tumor-to-brain contrast was significantly superior compared with ^{123}I-IMT SPECT scans, the results are encouraging for further evaluation of ^{18}F-FET for imaging brain tumors.

Key Words: *O*-(2-^{18}F-fluoroethyl)-L-tyrosine; 3-^{123}I-iodo-α-methyl-L-tyrosine; PET; SPECT; brain tumor

J Nucl Med 2004; 45:374–381

Metabolic imaging of brain tumors with radiolabeled amino acids has been shown to be a valuable method to improve the diagnostic accuracy in combination with anatomic radiologic methods (*1,2*). So far, the most commonly used amino acid tracers are ^{11}C-methyl-L-methionine (^{11}C-MET) for PET and 3-^{123}I-iodo-α-methyl-L-tyrosine (^{123}I-IMT) for SPECT (*2,3*).

Several studies have demonstrated that ^{11}C-MET PET allows a more accurate delineation of infiltrating gliomas than CT and MRI and is a sensitive method for the detection of tumor recurrences and for differentiation of brain tumors from nonneoplastic lesions (*4–8*). However, the short physical half-life of ^{11}C (20 min) necessitates an on-site cyclotron for ^{11}C-MET PET examinations and, therefore, the method remains limited to a few centers despite convincing scientific and clinical results.

SPECT with ^{123}I-IMT was introduced in neurooncology in 1989 (*9,10*) and has attracted considerable interest as an alternative to ^{11}C-MET PET for the investigation of cerebral gliomas (*3,11*). Although radiosynthesis of ^{123}I-IMT is not complex and SPECT facilities are widely available, the method is encumbered by some disadvantages: The availability of ^{123}I is limited in some countries, the labeling with ^{123}I is rather costly, and the favorable spatial resolution of PET cannot be achieved by SPECT.

To overcome the stated disadvantages of ^{11}C-MET PET and ^{123}I-IMT SPECT, several attempts have been undertaken to introduce an ^{18}F-labeled amino acid (110-min half-life) (*12,13*). Recently, ^{18}F-labeled amino acids have been developed that can be synthesized with high radiochemical yields, allowing large-scale production for clinical purposes (*14–16*). A very promising ^{18}F-labeled amino acid tracer is *O*-(2-^{18}F-fluoroethyl)-L-tyrosine (^{18}F-FET) (*15,16*). The first

Received Jun. 17, 2003; revision accepted Nov. 10, 2003.
For correspondence contact: Dirk Pauleit, MD, Clinic for Nuclear Medicine, Research Center Jülich, P.O. Box 1913, 52425 Jülich, Germany.
E-mail: pauleit@web.de

clinical studies using ^{18}F-FET in brain tumors were encouraging (*17*,*18*). The initial comparison of ^{18}F-FET and ^{11}C-MET imaging in patients with brain tumors showed a significant correlation of tumor-to-brain ratios (TBRs) and comparable intracerebral kinetics for both tracers (*19*). Similar transport characteristics for ^{18}F-FET and ^{11}C-MET were demonstrated in studies using F98 rat glioma cells (*20*).

Until now, a direct comparison of ^{123}I-IMT and ^{18}F-FET has not been performed. On the one hand, some results indicated a similar metabolic behavior for both tyrosine derivatives (*2*) but, on the other hand, differences in the biodistribution of these tracers in whole-body examinations were apparent (*21*,*22*). It appears to be reasonable to clarify whether the biologic distribution of ^{18}F-FET is similar to that of the established amino acid ^{123}I-IMT in brain tumors. In the case of comparable results, the rich clinical experience of ^{123}I-IMT might be directly applicable to the interpretation of ^{18}F-FET PET results.

Thus, the purpose of this study was to directly compare intratumoral, intracerebral, and extracerebral cranial accumulation of ^{123}I-IMT and ^{18}F-FET in a series of patients with brain tumors using state-of-the-art image fusion techniques with MRI.

MATERIALS AND METHODS

Patients

In a prospective study, 20 patients (mean age, 53 ± 11 y) with suspected brain tumors underwent ^{18}F-FET PET, ^{123}I-IMT SPECT, and MRI within 3 wk (mean, 6.3 ± 7.1 d). The examinations were performed before surgery or biopsy at the Department of Neurosurgery, University Hospital Düsseldorf. Except in one patient with a suspected cavernoma, all diagnoses were proven by histology. Individual data of the patients are given in Table 1. The examinations were approved by the university ethics committee and federal authorities. All subjects gave written informed consent for participation in the study.

Radiosynthesis of ^{18}F-FET and ^{123}I-IMT

The amino acid derivative ^{18}F-FET was produced via phase-transfer–mediated nucleophilic ^{18}F-fluorination of *N*-trityl-*O*-(2-tosyloxyethyl)-L-tyrosine tert-butyl ester and subsequent deprotection with a specific radioactivity of >200 GBq/μmol by optimizing the previously published method (*15*). The uncorrected radiochemical yield was about 35% and the radiochemical purity was >98%. The tracer was administered as an isotonic neutral solution.

^{123}I-IMT was prepared, as previously described, with a specific activity of >170 GBq/μmol (*23*).

PET, SPECT, and MRI

All patients remained fasting for at least 12 h before the PET and SPECT studies. PET studies were acquired 15–40 min after intravenous injection of 200 MBq ^{18}F-FET. The measurements were performed on an ECAT EXACT HR+ scanner (Siemens Medical Systems, Inc.) in 3-dimensional (3D) mode (32 rings; axial field of view, 15.5 cm). For attenuation correction, transmission scans with 3 ^{68}Ge/^{68}Ga rotating line sources were measured. After correction for random and scattered coincidences and dead time, image data were obtained by filtered backprojection in Fourier space as it is used in the ECAT 7.2 software (Direct inverse Fourier Transformation [DiFT]; Shepp filter, 2.48 mm [full width

TABLE 1
Patient Data

Patient no.	Age (y)	Sex	Diagnosis	Pretreatment	MRI*
1	37	F	Oligoastrocytoma WHO III	None	Gd−
2	45	F	Astrocytoma WHO II	None	Gd+
3	60	F	Demyelinization	None	Gd+
4	70	M	Oligodendroglioma WHO III	Surgery	Gd++; necrotic
5	33	M	Oligoastrocytoma WHO III	None	Gd+
6	50	F	Astrocytoma WHO III	None	Gd−
7	47	F	Cavernoma	None	Gd++
8	48	M	Astrocytoma WHO III	Surgery	Gd+
9	58	F	Glioblastoma WHO IV	None	Gd++
10	61	F	Astrogliosis	Biopsy	Gd−
11	57	F	Astrocytoma WHO II	None	Gd−
12	66	M	Astrocytoma WHO III	None	Gd++
13	54	M	Glioblastoma WHO IV	Surgery, irradiation	Gd++; necrotic
14	56	F	Oligodendroglioma WHO III	None	Gd+
15	49	F	Glioblastoma WHO IV	None	Gd++; necrotic
16	36	M	Oligodendroglioma WHO II	Surgery	Gd−
17	52	M	Astrocytoma WHO II	Surgery	Gd−
18	50	F	Astrogliosis	None	Gd−
19	74	F	Astrocytoma WHO II	None	Gd−
20	57	F	Oligodendroglioma WHO III	None	Gd+

*MRI shows no (Gd−), moderate (Gd+), or strong enhancement (Gd++) of gadolinium-labeled diethylenetriaminepentaacetic acid; necrotic = tumor has necrotic or cystoid components.
WHO = World Health Organization grade.

at half maximum]; pixel size, 2 × 2 × 2.4 mm^3). The reconstructed images were decay corrected; the reconstructed image resolution was about 5.5 mm.

Thirty minutes before administration of the ^{123}I-labeled amino acid, patients received 900 mg sodium perchlorate to prevent thyroidal uptake of free radioactive iodide. Fifteen to 40 min after injection of 400-MBq ^{123}I-IMT, SPECT data were acquired. The SPECT studies were performed using a triple-head γ-camera system (Triad 88; TRIONIX) equipped with ultra-high-resolution fanbeam collimators. The SPECT data (axial field of view, 23 cm; matrix, 64 × 64; pixel size, 3.56 × 3.56 mm) were reconstructed by filtered backprojection using a Butterworth filter (0.35 high cut, 3.0 rolloff) and corrected for attenuation according to Chang (*24*) (first order μ, 0.1 cm^{-1}) using a contour-finding procedure. The resolution of the reconstructed images was approximately 14 mm.

MR images were obtained with a 1.5-T system (Sonata; Siemens). For anatomic coregistration, a T1-weighted 3D Magnetization-prepared Rapid Acquisition Gradient Echo (MPRAGE) sequence (axial field of view, 25 cm; matrix, 205 × 256; repetition time, 11.4 s; echo time, 4.4 s; flip angle, 15°; number of slices, 128; slice thickness, 1.25 mm; number of averages, 1; time of acquisition, 6:02 min) was used in all patients.

Data Analysis

For coregistration, ^{18}F-FET PET, ^{123}I-IMT SPECT, and MRI data were transferred to the MPI-tool software package (version 3.28; ATV Advanced Tomo Vision), which was developed and described in detail by Pietrzyk et al. (*25*).

For visual analysis, identically resliced ^{18}F-FET PET and ^{123}I-IMT SPECT scans were independently evaluated by 3 observers who were unaware of clinical data. The presence of a brain tumor with abnormal tracer uptake was rated according to the following scoring scale: 1, definitely not present; 2, probably not present; 3, probably present; 4, definitely present. Additionally, the discrimination of anatomic brain structures (brain stem, cerebellum, caput nuclei caudate, thalamus, hippocampus, postcentral gyrus) on ^{18}F-FET PET and ^{123}I-IMT SPECT images was rated by the observers in a subjective manner using the following rating scale: 4, very good; 3, good; 2, fair; 1, poor.

κ-Statistics were used to measure the degree of agreement among the observers. κ-Values > 0 were considered to indicate positive correlation; values between 0 and 0.3, positive but poor correlation; values of 0.31–0.6, good correlation; values of 0.61–0.9, very good correlation; and values > 0.9, excellent correlation. For statistical comparison, the Wilcoxon signed rank test was performed using the mean scores of the 3 observers for the discrimination of anatomic structures and for the identification of brain tumors.

For semiquantitative analysis, the reconstructed ^{18}F-FET PET scans were filtered by using a Gauss filter (σ, 2.75 pixel), and the resolution was adapted to that of the ^{123}I-IMT SPECT scans.

Regions of interest (ROIs) were drawn manually over the brain tumors and the contralateral brain on coregistered PET and SPECT scans, avoiding cystic and necrotic tumor components according to the corresponding MRI scan. For determination of the normal brain activity, an ROI similar to the ROI of the brain lesion was placed in the contralateral hemisphere, obviously not affected. The TBR was calculated by dividing the mean activity of the ROI over the brain tumor and that of the normal brain. Additionally, ROIs were drawn over the superior sagittal sinus, the temporal muscle, and the cerebellum on MRI scans, and the anatomically adapted ROIs were transferred to the coregistered PET and SPECT scans for tracer uptake quantifications. Mean values of the ROIs were used for determination of the sinus-to-brain ratio (SBR), the cerebellum-to-brain ratio (CerBR), and the muscle-to-brain ratio (MBR).

Data were tested for normal distribution by the Kolmogorov–Smirnov test, and differences between the ^{18}F-FET and ^{123}I-IMT ratios were analyzed by the paired Student *t* test. Correlation analyses were performed by using the Pearson correlation coefficients. All statistical tests were considered significant at $P < 0.05$.

RESULTS

Semiquantitative Comparison of ^{18}F-FET and ^{123}I-IMT Uptake

The accumulation of ^{18}F-FET and ^{123}I-IMT in cerebral tumors demonstrated a close correlation ($r = 0.96$; $P < 0.001$) of the brain-to-brain ratios (TBR) (Fig. 1). The contrast between tumor and normal brain was significantly superior on ^{18}F-FET PET scans as compared with ^{123}I-IMT SPECT scans; the TBR for ^{18}F-FET was 2.0 ± 0.9 and for ^{123}I-IMT was 1.5 ± 0.5 ($P < 0.001$). For both tracers, the accumulation in the cerebellum was slightly higher than that in the supratentorial brain (CerBR ^{18}F-FET, 1.2 ± 0.1; CerBR ^{123}I-IMT, 1.3 ± 0.1).

In contrast to the findings in brain tumors, ^{18}F-FET and ^{123}I-IMT demonstrated obvious differences in extracerebral tissues. On ^{18}F-FET PET scans, the radioactivity in the muscles and the blood was higher compared with that in the normal brain. In contrast, on ^{123}I-IMT SPECT images, the radioactivity in the muscles and the blood was lower than that in the brain.

Significant correlations of the ^{18}F-FET and ^{123}I-IMT accumulation were not identified for skeletal muscles (r =

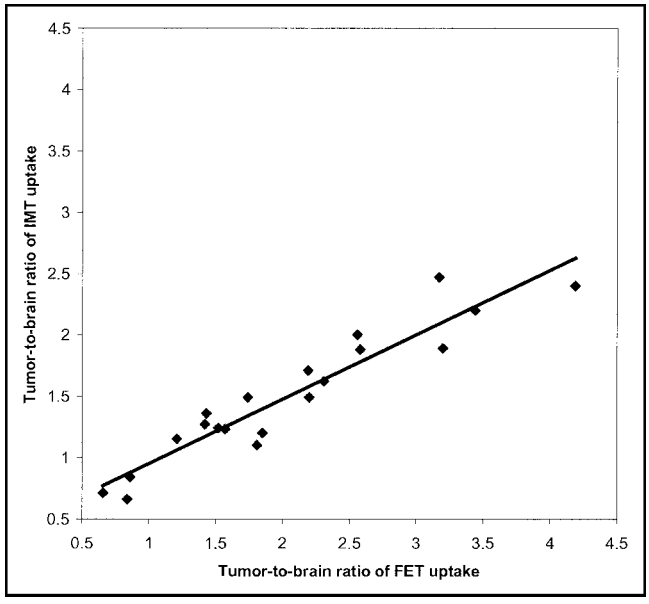

FIGURE 1. Comparison of TBRs for ^{18}F-FET PET and ^{123}I-IMT SPECT demonstrated a highly significant correlation ($r = 0.96$; $P < 0.001$).

−0.06; $P = 0.76$) or for blood-pool radioactivity ($r = 0.08$; $P = 0.80$). The accumulation of ^{18}F-FET in the temporal muscle was significantly higher compared with that of ^{123}I-IMT (MBR ^{18}F-FET, 1.4 ± 0.3; MBR ^{123}I-IMT, 0.6 ± 0.2; $P < 0.001$). Furthermore, radioactivity in the superior sagittal sinus was significantly higher for ^{18}F-FET than that for ^{123}I-IMT (SBR ^{18}F-FET, 1.3 ± 0.2; SBR ^{123}I-IMT, 0.8 ± 0.2; $P < 0.001$). The data of the calculated ratios are given in Table 2.

Visual Analysis of ^{18}F-FET PET and ^{123}I-IMT SPECT for Tumor Detection

The visual analysis of ^{18}F-FET PET and ^{123}I-IMT SPECT for the detection of brain tumors demonstrated a very good agreement (κ-value, 0.7 ± 0.1) among the 3 observers who were unaware of clinical data. The mean rating scores of the readers are also given in Table 2. The results yielded no substantial differences between ^{18}F-FET PET and ^{123}I-IMT SPECT. Figure 2 illustrates the ^{18}F-FET PET and ^{123}I-IMT SPECT scans of a 56-y-old woman with a malignant oligodendroglioma (World Health Organization grade III). The tumor was clearly identified on both ^{18}F-FET PET and ^{123}I-IMT SPECT and was rated as definitely present by all 3 observers. In 19 of 20 patients, results were consistent for the presence of tumor on the ^{18}F-FET PET scans and ^{123}I-IMT SPECT scans. No obvious discrepancies in the spread and shape of the tracer-accumulating tumor area were noted. Two of the patients with histologically proven brain tumors demonstrated no abnormal tracer uptake on both ^{18}F-FET PET scans and ^{123}I-IMT SPECT scans. Two other patients had positive ^{18}F-FET PET scans as well as positive ^{123}I-IMT SPECT scans, and subsequent histology revealed astrogliosis in one case; in the second patient, a biopsy was not performed because of a suspected cavernoma.

In only one patient with a low-grade glioma was the tumor identified on the ^{18}F-FET PET scans but not on the ^{123}I-IMT SPECT scans by the 3 observers (Fig. 3). The corresponding semiquantitative analysis revealed a lower contrast between tumor and normal brain on ^{123}I-IMT SPECT (TBR, 1.1) compared with ^{18}F-FET PET (TBR, 1.8) in this patient.

In the Wilcoxon signed rank test, no significant difference was found for tumor detection comparing the rating scores of ^{18}F-FET PET (mean, 3.3 ± 1.1) and ^{123}I-IMT SPECT (mean, 3.0 ± 1.1).

TABLE 2
Rating Scores for Presence of Brain Tumors on ^{18}F-FET PET and ^{123}I-IMT SPECT and Calculated Ratios for ^{18}F-FET and ^{123}I-IMT Uptake in Brain Tumors, Superior Sagittal Sinus, Temporalis Muscle, and Cerebellum

Patient no.	Mean rating score		TBR		SBR		MBR		CerBR	
	^{18}F-FET	^{123}I-IMT	^{18}F-FET	^{123}I-IMT	^{18}F-FET	^{123}I-IMT	^{18}F-FET	^{123}I-IMT	^{18}F-FET	^{123}I-IMT
1	4	3	2.2	1.5	1.5	1.0	1.9	0.7	1.3	1.3
2	4	3	2.2	1.7	1.0	0.9	1.3	0.9	1.2	1.3
3	1	1	0.8	0.7	1.5	0.8	1.7	0.9	1.2	1.4
4	4	4	4.2	2.4	1.4	1.0	1.2	0.5	1.2	1.3
5	4	3	1.5	1.2	1.5	0.7	1.6	0.5	1.3	1.3
6	1	2	0.9	0.8	1.3	0.9	1.1	0.6	1.2	1.4
7	3	3	1.4	1.4	1.1	0.8	1.3	0.5	1.2	1.4
8	4	4	2.6	2.0	1.1	1.1	1.2	0.7	1.0	1.2
9	4	4	3.2	2.5	1.0	0.4	1.3	0.4	1.0	1.2
10	3	3	1.6	1.2	1.7	0.7	1.5	0.6	1.2	1.4
11	4	1	1.8	1.1	1.0	0.9	1.0	0.9	1.1	1.4
12	4	4	2.3	1.6	1.0	0.7	1.3	0.4	1.2	1.2
13	2	2	1.4	1.3	1.2	0.6	1.5	0.8	1.3	1.3
14	4	4	3.4	2.2	1.3	0.8	1.7	0.7	1.3	1.3
15	4	3	1.9	1.2	1.3	0.8	1.3	0.7	1.1	1.2
16	4	4	2.6	1.9	1.2	0.8	1.1	0.5	1.4	1.4
17	1	1	0.7	0.7	1.1	0.7	1.3	0.6	1.2	1.3
18	2	2	1.2	1.2	1.2	1.1	1.0	0.6	1.2	1.3
19	4	4	1.7	1.5	1.5	0.8	1.8	0.5	1.3	1.4
20	4	4	3.2	1.9	1.4	0.7	1.3	0.5	1.1	1.2
Mean	3.3	3.0	2.0	1.5	1.3	0.8	1.4	0.6	1.2	1.3
SD	1.1	1.1	0.9	0.5	0.2	0.2	0.3	0.2	0.1	0.1
	NS		$P < 0.001$		$P < 0.001$		$P < 0.001$		$P < 0.001$	
Pearson correlation coefficient			$r = 0.96$ $P < 0.001$		$r = 0.08$ NS		$r = -0.06$ NS		$r = 0.55$ $P = 0.02$	

NS = not significant.
Mean rating score: 1, definitely not present; 2, probably not present; 3, probably present; 4, definitely present.

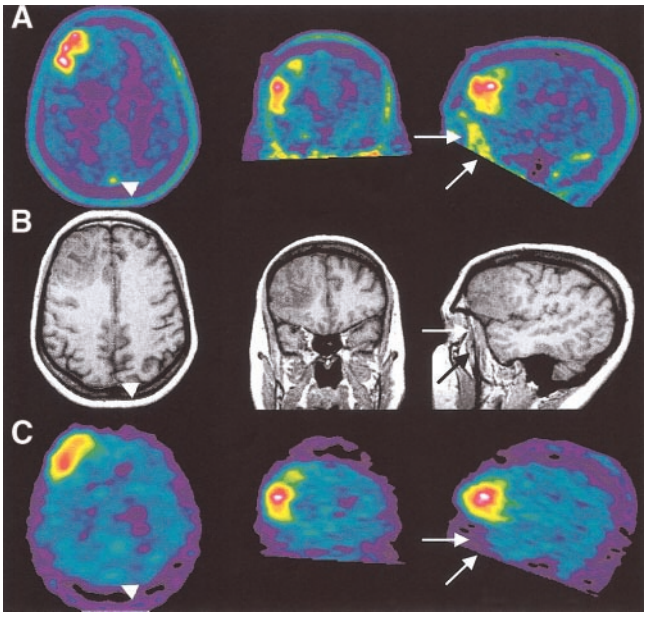

FIGURE 2. Coregistered ^{18}F-FET PET, ^{123}I-IMT SPECT, and MRI of 56-y-old woman with a malignant oligodendroglioma (patient 14) in the right frontal lobe. The tumor was clearly identified on ^{18}F-FET PET and ^{123}I-IMT SPECT and was rated as definitely present by all 3 observers. The TBR was 3.4 for ^{18}F-FET PET scans and was 2.2 for ^{123}I-IMT SPECT scans. On PET images, the accumulation of ^{18}F-FET was higher in the superior sagittal sinus (arrowhead) and in the temporal muscle (arrows) compared with that on the ^{123}I-IMT SPECT images. (A) ^{18}F-FET PET. (B) MRI. (C) ^{123}I-IMT SPECT.

Visual Analysis of Anatomic Structures

The discrimination of the anatomic intracerebral structures (brain stem, cerebellum, caput nuclei caudate, thalamus, hippocampus, postcentral gyrus) was significantly superior on ^{18}F-FET PET scans as compared with that on the ^{123}I-IMT SPECT scans. The mean scores for the ^{18}F-FET PET and ^{123}I-IMT SPECT scans were 2.6 ± 0.9 and 1.7 ± 0.9, respectively ($P < 0.001$). On the ^{18}F-FET PET scans, the identification of the cerebellum, brain stem, caput nuclei caudate, and thalamus was rated good to very good, the discrimination of the hippocampus was rated fair, and that of the postcentral gyrus was poor. In contrast, on ^{123}I-IMT SPECT scans, only the identification of the cerebellum was rated good to very good. Detailed data are given in Table 3. The observers demonstrated good agreement in the rating scores (κ-value, 0.34 ± 0.15).

DISCUSSION

In this study the cranial distribution of ^{18}F-FET and ^{123}I-IMT uptake was directly compared in a series of patients with brain tumors.

Intratumoral tracer distribution was similar for ^{18}F-FET and ^{123}I-IMT and a strong and significant correlation ($r = 0.96$) of the TBRs was found (Figs. 1 and 2). The mean TBRs, however, were significantly higher for ^{18}F-FET than for ^{123}I-IMT. A direct comparison of ^{18}F-FET PET and ^{123}I-IMT SPECT has not yet been performed, but our results are in agreement with studies comparing ^{18}F-FET and ^{11}C-MET uptake, on the one hand, and ^{123}I-IMT and ^{11}C-MET uptake, on the other hand (*19*,*26*).

Comparing ^{18}F-FET and ^{11}C-MET, a close correlation ($r = 0.98$) was reported in patients with brain tumors (*19*), and the TBRs of both tracers were in the same range. This observation was confirmed by dual-tracer autoradiography in experimental rat gliomas (*20*).

Also, studies comparing ^{11}C-MET PET and ^{123}I-IMT SPECT in patients with brain tumors as well as in experimental animal studies demonstrated a significant correlation of the TBRs of ^{11}C-MET and ^{123}I-IMT (*26*,*27*). In these studies, consistently higher TBRs for ^{11}C-MET than for ^{123}I-IMT have been reported, which is in agreement with the findings of the present study.

It was speculated that differences in the lipophilicity of the tracers may account for this phenomenon (*27*). However, another factor that contributes to the lower TBRs in ^{123}I-IMT SPECT is the faster washout of ^{123}I-IMT from the tumor tissue as compared with ^{11}C-MET and ^{18}F-FET, respectively. This leads to a decrease of the TBRs of about 20% from 15 to 60 min after injection in ^{123}I-IMT SPECT (*26*). In contrast, the ^{18}F-FET concentration in the tumor and normal brain tissue remains rather constant within this period of time (*19*).

Uptake of ^{18}F-FET and ^{123}I-IMT is mediated by specific amino acid transporters, but both amino acids are not incorporated into proteins (*3*,*19*). Several studies have analyzed the transport mechanisms of ^{123}I-IMT and demon-

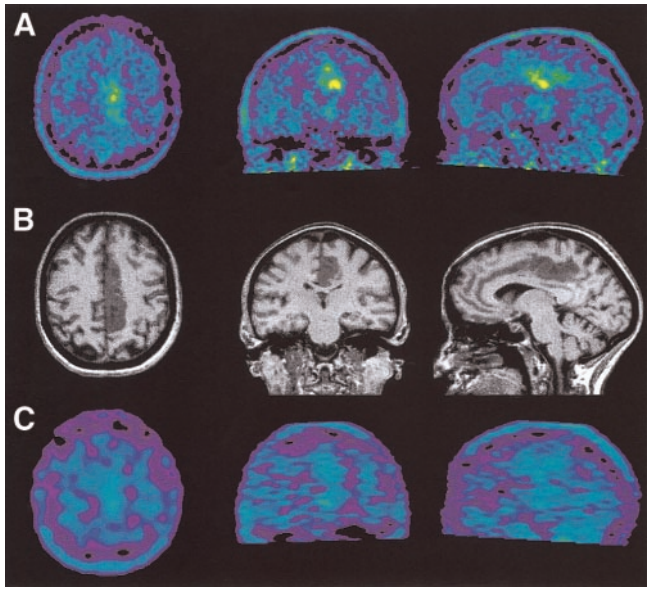

FIGURE 3. Coregistered ^{18}F-FET PET, ^{123}I-IMT SPECT, and MRI of 57-y-old woman with a low-grade astrocytoma (patient 11) in the posterior cingulum. The tumor was identified on ^{18}F-FET PET but not on the ^{123}I-IMT SPECT images by the 3 observers. The TBR was 1.8 for ^{18}F-FET PET and was 1.1 for ^{123}I-IMT SPECT. (A) ^{18}F-FET PET. (B) MRI. (C) ^{123}I-IMT SPECT.

TABLE 3
Discrimination of Anatomic Structures on ^{18}F-FET PET and ^{123}I-IMT SPECT Scans (n = 20)

	^{18}F-FET PET					^{123}I-IMT SPECT				
Anatomic structure	1	2	3	4	Mean score	1	2	3	4	Mean score
Cerebellum	0/20	1/20	5/20	14/20	3.7	2/20	1/20	10/20	7/20	3.1
Brain stem	1/20	4/20	11/20	4/20	2.9	7/20	8/20	4/20	1/20	2.0
Caput nuclei caudate	1/20	4/20	12/20	3/20	2.9	15/20	4/20	1/20	0/20	1.3
Thalamus	1/20	3/20	11/20	5/20	3.0	10/20	8/20	2/20	0/20	1.5
Hippocampus	2/20	14/20	4/20	0/20	2.1	20/20	0/20	0/20	0/20	1.0
Gyrus postcentralis	14/20	6/20	0/20	0/20	1.4	20/20	0/20	0/20	0/20	1.0
Total					2.6 ± 0.9					1.7 ± 0.9

Mean scores of 3 observers were used: 4, very good; 3, good; 2, fair; 1, poor.

strated concordantly a specific transport dominated by sodium-independent transport system L (*3*). The similarity of the transport characteristics of ^{123}I-IMT to those of ^{11}C-MET has been shown in human glioma cells (*28*). For ^{18}F-FET, data on transport mechanisms are sparse. Initial studies demonstrated a 24-fold higher uptake of L-FET compared with the D-isomer in the brain of nude mice, indicating stereoselective transport (*16*). A 70% reduction of ^{18}F-FET transport was observed in SW 707 colon carcinoma cells using 2-aminobicyclo-2,2,1-heptane-2-carboxylic acid as an inhibitor of system L amino acid transport, but Na^+ dependence of transport was not evaluated (*29*). Transport experiments with ^{18}F-FET in F98 rat glioma cells revealed a sodium-dependent transport via system $B^{0,+}$ in addition to sodium-independent transport via system L, but the transport characteristics of ^{18}F-FET in this specific cell line were nearly identical to those of ^{11}C-MET (*20*). Thus, the similarities of transport mechanisms for ^{123}I-IMT and ^{11}C-MET, on the one hand, and of ^{18}F-FET and ^{11}C-MET, on the other hand, are well documented and are in agreement with imaging results of cerebral gliomas.

The comparability of ^{18}F-FET and ^{123}I-IMT uptake in brain tumors is further supported by the qualitative analysis by the 3 independent observers. This additional visual analysis of ^{18}F-FET PET and ^{123}I-IMT SPECT images is rather close to the clinical setup since diagnostic evaluation is usually done by qualitative scan reading. Overall, a very good agreement between the 3 observers was achieved. ^{18}F-FET PET and ^{123}I-IMT SPECT scans yielded consistent results in 19 of 20 patients with regard to the presence or absence of brain tumors. In one patient, the tumor was only identified on the ^{18}F-FET PET images. The lower contrast between tumor and normal brain in ^{123}I-IMT SPECT (TBR, 1.1) compared with the that in ^{18}F-FET PET (TBR, 1.8) may account for this difference (Fig. 3).

In general, the findings of our study and that of previous studies (*19*,*26*) suggest that clinical experience with ^{123}I-IMT SPECT as well as with that of ^{11}C-MET PET can be used as a basis for the clinical interpretation of ^{18}F-FET PET studies in brain tumors.

The potential of radiolabeled amino acids for the diagnostic evaluation of brain tumors has been demonstrated in numerous studies (*2*,*3*). One of the main advantages of using amino acids appears to be the visualization of the true tumor extent of gliomas (*6*,*7*,*11*). Although CT and MRI are unsurpassed diagnostic modalities for the detection of cerebral space-occupying lesions, the differentiation of tumor tissue from nontumorous tissue, such as perifocal edema, is difficult with these morphologic methods (*30*). Although unspecific uptake of amino acids may not be excluded, ^{11}C-MET and ^{123}I-IMT uptake appears to be sensitive to differentiate high-grade gliomas from nontumorous lesions (*8*) and recurrences from scarring (*7*,*31*) and to monitor therapeutic effects (*32*).

For ^{11}C-MET it has been demonstrated that uptake within the limit of the tumor is related to the local level of malignancy as estimated histologically on stereotactic biopsies (*33*). This is of importance considering the high level of regional heterogeneity of gliomas and the potential benefit of ensuring the resection or destruction of most malignant components of the tumor when complete resection cannot be performed without unacceptable morbidity. Such a metabolically guided resection has proved feasible using stereotactic ^{11}C-MET PET information to direct resection of brain tumor under neuronavigation (*34*).

The role of radiolabeled amino acids for the determination of tumor grading of cerebral gliomas is controversial. In a larger series of patients, a difference in ^{11}C-MET uptake between high-grade and low-grade gliomas was shown, but the overlap of the 2 groups was too high to predict grading precisely in individual tumors (*8*). For ^{123}I-IMT, some authors observed a high accuracy of ^{123}I-IMT SPECT for the separation of high-grade from low-grade gliomas, but others could not identify such a difference and observed a wide overlap of ^{123}I-IMT uptake in different tumor grades (*3*). Similarly, L-1-^{11}C-tyrosine PET revealed no correlation between histologic grading and proliferative activity of human brain tumors (*35*). With regard to ^{18}F-FET PET, our database is still too small to draw any conclusions. The meaning of amino acid uptake in gliomas for the prediction of prog-

nosis is still under investigation. One study reported significantly longer survival times for glioma patients with low ^{11}C-MET uptake than for glioma patients with high ^{11}C-MET uptake (*36*). In low-grade gliomas, ^{11}C-MET uptake was a good prognostic indicator (*37*). ^{123}I-IMT uptake appears not to be an indicator of survival time in patients with gliomas (*1*), but the extent of the lesion on ^{123}I-IMT SPECT was an independent predictor of prognosis (*38*). Also, after resection of primary brain tumors, significantly longer survival times in patients without ^{123}I-IMT uptake than in patients with residual ^{123}I-IMT uptake were reported (*39*). However, these data likely reflect the known influence of total tumor resection on the prognosis of patients with cerebral gliomas, rather than that they support the predictive value of ^{123}I-IMT uptake for individual prognosis. Thus, these particular studies confirm the potential of amino acids for the identification of residual tumor tissue. It appears that imaging of gliomas with radiolabeled amino acids—^{11}C-MET, ^{123}I-IMT, or ^{18}F-FET—yields most benefit concerning the identification of glioma tissue, which is helpful for therapy planning (surgery, radiotherapy), detection of recurrence, identification of an optimal biopsy site, and therapy control. Histologic grading of individual tumors or prediction of survival time for ^{18}F-FET PET needs further investigation but appears to be inferior to that of ^{18}F-FDG PET.

Since PET provides a considerable higher spatial resolution than SPECT, the discrimination of anatomic brain structures was significantly superior on ^{18}F-FET PET scans compared with that on the ^{123}I-IMT SPECT scans. This is an important advantage of ^{18}F-FET PET that allows improved description of the tumor location. Moreover, it facilitates image coregistration with morphologic data such as MRI and clinical acceptance. For both tracers the accumulation in the cerebellum was slightly higher than that in the supratentorial brain (CerBR ^{18}F-FET, 1.2 ± 0.1; CerBR ^{123}I-IMT, 1.3 ± 0.1) and a significant positive correlation of the TBRs was identified for ^{18}F-FET and ^{123}I-IMT. This finding supports the hypothesis that the physiologic behavior of ^{18}F-FET and ^{123}I-IMT is similar within the brain. SPECT is still more widely available than PET but the ^{123}I tracer are very costly and disposability is not better than that of ^{18}F tracers. Since, for ^{123}I-IMT studies, a relatively high tracer dose is needed, the total costs of an ^{123}I-IMT SPECT study are similar to those of a ^{18}F-FET PET study. Thus, ^{18}F-FET PET should become the method of choice when a PET scanner is available while ^{123}I-IMT SPECT remains a useful alternative in hospitals without a PET facility.

In contrast to the findings in brain tumors, ^{18}F-FET and ^{123}I-IMT demonstrated obvious differences concerning the uptake in extracerebral tissues. The higher radioactivity of ^{18}F-FET in the muscles and the blood compared with the normal brain tissue was previously reported (*22*). The blood-pool radioactivity of ^{18}F-FET visualizes large cerebral vessels that may be a disadvantage of ^{18}F-FET but can be overcome by performing late ^{18}F-PET scans. Since the radioactivity increases in the normal brain over time, similar levels of radioactivity in the blood and the brain are usually reached on late scans 1 h after injection of ^{18}F-FET (*22*). The higher blood-pool radioactivity of ^{18}F-FET may be attributed to the low urinary excretion of ^{18}F-FET, which is only 22% of the injected activity after 5 h (*22*). This is relatively low compared with ^{123}I-IMT, which exhibited a 75% urinary excretion after 5 h (*21*).

The reasons for the different physiologic behavior and transport characteristics of ^{18}F-FET and ^{123}I-IMT in extracerebral tissues remain to be explored. In principle, it has been shown that even minimal structural differences in radioloabeled amino acids result in completely different biokinetics (*1*). Recently, the transport selectivity of ^{123}I-IMT for the isoform of human L-type amino acid transporter hLAT1 was detected while the natural parent L-tyrosine was transported by hLAT1 and hLAT2 (*40*). The emerging interest of molecular biologic sciences in nuclear medicine may provide a more specific characterization of new radiolabeled amino acids in the near future.

CONCLUSION

^{18}F-FET and ^{123}I-IMT demonstrated similar uptake in brain tumors, and the TBRs of both tracers showed a significant strong correlation in this initial evaluation with a relatively limited number of patients. It is expected that the clinical experience with ^{123}I-IMT SPECT in the diagnosis and follow-up of brain tumors will be valid for ^{18}F-FET PET. However, this must be addressed in a larger series of patients with nonneoplastic lesions and patients who had undergone previous therapy.

As ^{18}F-FET PET allows improved discrimination of anatomic structures and the tumor-to-brain contrast was significantly superior compared with ^{123}I-IMT SPECT scans, the results are encouraging for further evaluation of ^{18}F-FET for imaging brain tumors.

ACKNOWLEDGMENT

The authors thank Elisabeth Theelen, Suzanne Schaden, and Heike Friedrich for assistance in patient studies and data analysis and Bettina Palm, Erika Wabbals, Silke Grafmüller, Johannes Ermert, and Sascha Rehbein for radiosynthesis of the tracer and technical assistance. The facility for MRI used in this study was supported by the Bundesministerium für Bildung und Forschung (grant BMBF 01GO0104).

REFERENCES

1. Langen KJ. Amino acid transport studies in brain tumors. In: Feinendegen LE, Shreeve WW, Eckelman WC, Bahk YW, Wagner HN Jr, eds. *Molecular Nuclear Medicine: The Challenge of Genomics and Proteomics to Clinical Practice.* New York, NY: Springer-Verlag; 2003:477–485.
2. Jager PL, Vaalburg W, Pruim J, de Vries EG, Langen KJ, Piers DA. Radiolabelled amino acids: basic aspects and clinical applications in oncology. *J Nucl Med.* 2001;42:432–445.
3. Langen KJ, Pauleit D, Coenen HH. 3[^{123}I]Iodo-alpha-methyl-L-tyrosine: uptake mechanisms and clinical applications. *Nucl Med Biol.* 2002;29:625–631.
4. Bergström M, Collins VP, Ehrin E, et al. Discrepancies in brain tumor extent as

shown by computed tomography and positron emission tomography using [^{68}Ga] EDTA, [^{11}C] glucose, and [^{11}C] methionine. *J Comput Assist Tomogr.* 1983;7: 1062–1066.
5. Mosskin M, Ericson K, Hindmarsh T, et al. Positron emission tomography compared with magnetic resonance imaging and computed tomography in supratentorial gliomas using multiple stereotactic biopsies as reference. *Acta Radiol.* 1989;30:225–232.
6. Derlon JM, Bourdet C, Bustany P, et al. [^{11}C] L-methionine uptake in gliomas. *Neurosurgery.* 1989;25:720–728.
7. Ogawa T, Shishido F, Kanno I, et al. Cerebral glioma: evaluation with methionine PET. *Radiology.* 1993;186:45–53.
8. Herholz K, Holzer T, Bauer B, et al. ^{11}C-Methionine PET for differential diagnosis of low-grade gliomas. *Neurology.* 1998;50:1316–1322.
9. Biersack HJ, Coenen HH, Stöcklin G, et al. Imaging of brain tumors with L-3-[^{123}I]iodo-α-methyl tyrosine and SPECT. *J Nucl Med.* 1989;30:110–112.
10. Langen KJ, Coenen HH, Roosen N, et al. SPECT studies of brain tumors with L-3-[^{123}I]Iodo-α-methyl tyrosine: comparison with PET, ^{124}IMT and first clinical results. *J Nucl Med.* 1990;31:281–286.
11. Weckesser M, Schmidt D, Matheja P, Coenen HH, Langen KJ. The role of L-3-I-123-iodine-alpha-methyltyrosine SPECT in cerebral gliomas. *Nuklearmedizin.* 2000;39:233–240.
12. Coenen HH. Biochemistry and evaluation of fluoroamino acids. In: Mazoyer BM, Heiss WD, Comar D, eds. *PET Studies on Amino Acid Metabolism and Protein Synthesis.* London, U.K.: Kluwer Academic; 1993:109–129.
13. Laverman P, Boerman OC, Corstens FH, et al. Fluorinated amino acids for tumor imaging with positron emission tomography. *Eur J Nucl Med.* 2002;29:681–690.
14. Hamacher K. Synthesis of n.c.a. cis- and trans-4-[^{18}F]fluoro-L-proline, a radiotracer for PET-investigation of disordered matrix protein synthesis. *J Labelled Compds Radiopharm.* 1999;42:1135–1142.
15. Hamacher K, Coenen HH. Efficient routine production of the ^{18}F-labelled amino acid O-(2-[^{18}F]fluoroethyl)-L-tyrosine. *Appl Radiat Isot.* 2002;57:853–856.
16. Wester HJ, Herz M, Weber W, et al. Synthesis and radiopharmacology of O-(2-[^{18}F]fluoroethyl-L-tyrosine for tumor imaging. *J Nucl Med.* 1999;40:205–212.
17. Messing-Jünger AM, Floeth FW, Pauleit D, et al. Multimodal target point assessment for stereotactic biopsy in children with diffuse bithalamic astrocytomas. *Childs Nerv Syst.* 2002;18:445–449.
18. Pauleit D, Langen KJ, Floeth F, et al. Improved delineation of the tumor extension using [^{18}F]FET PET compared with MRI in cerebral gliomas [abstract]. *J Nucl Med.* 2002;43(suppl):112P.
19. Weber WA, Wester HJ, Grou AL, et al. O-(2-[^{18}F]fluoroethyl)-L-tyrosine and L-[methyl-^{11}C]methionine uptake in brain tumors: initial results of a comparative study. *Eur J Nucl Med.* 2000;27:542–549.
20. Langen KJ, Jarosch M, Mühlensiepen H, et al. Comparison of fluorotyrosines and methionine uptake in F98 rat gliomas. *Nucl Med Biol.* 2003;30:501–508.
21. Schmidt D, Langen KJ, Herzog H, et al. Whole-body kinetics and dosimetry of L-3-^{123}I-iodo-alpha-methyltyrosine. *Eur J Nucl Med.* 1997;24:1162–1166.
22. Pauleit D, Floeth F, Herzog H, et al. Whole-body distribution and dosimetry of O-(2-[^{18}F]fluoroethyl)-L-tyrosine (FET). *Eur J Nucl Med.* 2003;30:519–524.
23. Krummeich C, Holschbach M, Stöcklin G. Direct n.c.a. electrophilic radioiodination of tyrosine analogues: their in vivo stability and brain-uptake in mice. *Appl Radiat Isot.* 1994;45:929–935.
24. Chang LT. A method for attenuation correction in radionuclide computed tomography. *IEEE Trans Nucl Sci.* 1978;25:638–643.
25. Pietrzyk U, Herholz K, Heiss WD. Three-dimensional alignment of functional and morphological tomograms. *J Comput Assist Tomogr.* 1990;14:51–59.
26. Langen KJ, Ziemons K, Kiwit JC, et al. 3-[^{123}I]Iodo-alpha-methyltyrosine and [methyl-^{11}C]-L-methionine uptake in cerebral gliomas: a comparative study using SPECT and PET. *J Nucl Med.* 1997;38:517–522.
27. Langen KJ, Clauss RP, Holschbach M, et al. Comparison of iodotyrosines and methionine uptake in a rat glioma model. *J Nucl Med.* 1998;39:1596–1599.
28. Langen KJ, Mühlensiepen H, Holschbach M, et al. Transport mechanisms of 3-[^{123}I]iodo-α-methyl-L-tyrosine in a human glioma cell line: comparison with [^{3}H]methyl]-L-methionine. *J Nucl Med.* 2000;41:1250–1255.
29. Heiss P, Mayer S, Herz M, Wester HJ, Schwaiger M, Senekowitsch-Schmidtke R. Investigation of transport mechanism and uptake kinetics of O-(2-[^{18}F]fluoroethyl)-L-tyrosine in vitro and in vivo. *J Nucl Med.* 1999;40:1367–1373.
30. Leeds NE, Jackson EF. Current imaging techniques for the evaluation of brain neoplasms. *Curr Opin Oncol.* 1994;6:254–261.
31. Guth-Tougelidis B, Muller S, Mehdorn MM, Knust EJ, Dutschka K, Reiners C. Uptake of DL-3-^{123}I-iodo-alpha-methyltyrosine in recurrent brain tumors. *Nuklearmedizin.* 1995;34:71–75.
32. Floeth FW, Aulich A, Langen KJ, Burger KJ, Bock WJ, Weber F. MR imaging and single-photon emission CT findings after gene therapy for human glioblastoma. *AJNR.* 2001;22:1517–1527.
33. Goldman S, Levivier M, Pirotte B, et al. Regional methionine and glucose uptake in high-grade gliomas: a comparative study on PET-guided stereotactic biopsy. *J Nucl Med.* 1997;38:1459–1462.
34. Levivier M, Wikler D, Goldman S, et al. Positron emission tomography in stereotactic conditions as a functional imaging technique for neurosurgical guidance. In: Alexander EI, Maciunas RJ, eds. *Advanced Neurosurgical Navigation.* New York, NY: Thieme Medical Publishers; 1999:85–99.
35. de Wolde H, Pruim J, Mastik MF, Koudstaal J, Molenaar WM. Proliferative activity in human brain tumors: comparison of histopathology and L-[1-^{11}C]tyrosine PET. *J Nucl Med.* 1997;38:1369–1374.
36. Kaschten B, Stevenaert A, Sadzot B, et al. Preoperative evaluation of 54 gliomas by PET with fluorine-18-fluorodeoxyglucose and/or carbon-11-methionine. *J Nucl Med.* 1998;39:778–785.
37. Ribom D, Eriksson A, Hartman M, et al. Positron emission tomography ^{11}C-methionine and survival in patients with low-grade gliomas. *Cancer.* 2001;92: 1541–1549.
38. Weckesser M, Matheja P, Schwarzrock A, et al. Prognostic significance of amino acid transport imaging in patients with brain tumors. *Neurosurgery.* 2002;50: 958–964.
39. Weber WA, Dick S, Reidl G, et al. Correlation between postoperative 3-[^{123}I]iodo-L-α-methyltyrosine uptake and survival in patients with gliomas. *J Nucl Med.* 2001;42:1144–1150.
40. Shikano N, Kanai Y, Kawai K, et al. Isoform selectivity of 3-^{125}I-iodo-α-methyl-L-tyrosine membrane transport in human L-type amino acid transporters. *J Nucl Med.* 2003;44:244–246.